

Diagrid structures as innovative retrofit solutions for existing reinforced concrete buildings

Simone Labò, Chiara Passoni, Alessandra Marini, Andrea Belleri, Paolo Riva

*University of Bergamo,
Via Salvecchio 19, Bergamo 24129, Italy*

Abstract

In recent years the redevelopment of the post-World War II reinforced concrete heritage has become an essential action to meet energy-saving and to foster safety and resilience of European communities. In order to overcome the major barriers to the renovation, new solutions should follow a holistic approach, thus solving the structural, energy and architectural deficiency at the same time. The interventions should be carried out from outside the building, so as to leave the building use unaltered, with no need of user relocation, and Life Cycle Thinking (LCT) principles should be addressed. In this paper, these main pillars are translated into an innovative technology, the steel diagrid exoskeleton, for which a proportioning criterion is proposed, besides the assessment of its effectiveness as a seismic risk mitigation measure. Among possible structural typologies, diagrids are particularly interesting for their remarkable architectural potential and for the possible standardization of the components.

1 Introduction

A serious action must be undertaken for a deep renovation of the existing building stock. Earthquakes have caused millions of victims in the last 100 years, and the improvements in the design codes have only slightly reduced the dead toll. From a structural point of view, 40% of the European buildings have already exhausted their nominal structural service life of 50 years. Moreover, having been built before the 1970s, such buildings were often built without any seismic regulation and furthermore, the building collapse after a natural disaster has a great impact on the environment in terms of waste production and CO₂ emission [1]. Additionally, the existing building stock is liable for 40% of the EU energy consumption, it features obsolete envelopes and technologies, and is characterized by poor housing condition and living discomfort. The existing building stock is therefore obsolete, energy consuming and seismic vulnerable.

However, although the civil engineering community agrees on the necessity to develop a new approach for the building design and for preventing unnecessary future loss, only an average renovation rate of 1% [2] characterizes the building sector. In this context, the major barriers to the renovation are the inhabitants' relocation and the long downtime of the building, the high cost of the interventions and the lack of adequate business models fostering the renovation [3]. To overcome these barriers, integrated retrofit techniques are required to solve all the building deficiencies at one time. The intervention should be carried out from outside, avoiding the inhabitants' relocation and the building downtime [4]. Finally, in order to favor a sustainable retrofit solution, Life Cycle Thinking (LCT) principles should be considered. To this aim, prefabricated components, easily demountable, repairable and adaptable technologies using recyclable/reusable material should be preferred to increase the sustainability throughout the entire building life-cycle.

These considerations lead to a holistic and integrated approach that could be achieved with the innovative technology of the steel diagrid exoskeleton [5], which integrates the structural elements for the seismic upgrading with the new insulation and architectural layers. The diagrid structure is assembled from outside the building; standardization of the connections and light pre-fabrication of its components are compliant with LCT principles and may be conveniently adopted in incremental rehabilitation plans. On the basis of these considerations, a design method for diagrid structure as a retrofit solution for reinforced concrete buildings is proposed.

2 Diagrid design method

The structural design of buildings is becoming a very complex process, in which different criteria are taken into account, such as the structural interactions between the existing building and the additional retrofit structures, the use of eco-compatible materials, demountable technology, among many others. In the diagrid design method proposed hereafter focus is paid to 1) the geometry, which must meet architectural and aesthetic aspects; 2) the minimum stiffness guaranteeing the existing building safety; and 3) the maximum axial force in the diagrid diagonal elements as to avoid their buckling.

2.1 Geometry and loads

The optimal diagrid geometry is influenced by several parameters related to the existing structure layout and features and to the diagrid performances. As far as the existing building is concerned, the retrofitting diagrid has to comply with architectural and aesthetic needs, as well as its layout must enable possible envisioned living spaces expansion. The diagrid performances, instead, are strictly related to the inclination of the diagonal elements and, in general, the optimal angle is a function of the building height [6]; for example, past researches carried out on the use of diagrid structural systems in new high-rise buildings [7] show that 90° is the optimal angle, which ensures maximal flexural stiffness and 35° to provide maximum shear stiffness. Accordingly, for the integrated retrofit of low-medium rise buildings, an optimal reference angle of 35° should be considered, while also accounting for the geometry and the characteristics of the reference building.

The geometry of the module plays a fundamental role in the definition of the load pattern and the internal forces [8]. The module is composed of two diagonal and one horizontal elements. First of all, as far as the load pattern is concerned, horizontal loads and vertical loads are analyzed separately. Assuming that the system behavior is governed by the external diagrid, a linear distribution of the seismic loads is considered. The gravity loads are represented by vertical loads at each node of the diagrid [6], [7]. In the particular case of use of diagrids as retrofit measure, diagrid exoskeletons are subject to their self-weight, while they do not withstand the existing building vertical load. Finally, by decoupling bending and shear and by assuming that the bending moment is resisted by the diagrid facades orthogonal to the seismic action (“flange” facades), whilst the shear force is counteracted by the diagrid facades parallel to the seismic action (“web” facades), the diagrid internal forces can be evaluated as shown in Figure 2 [9].

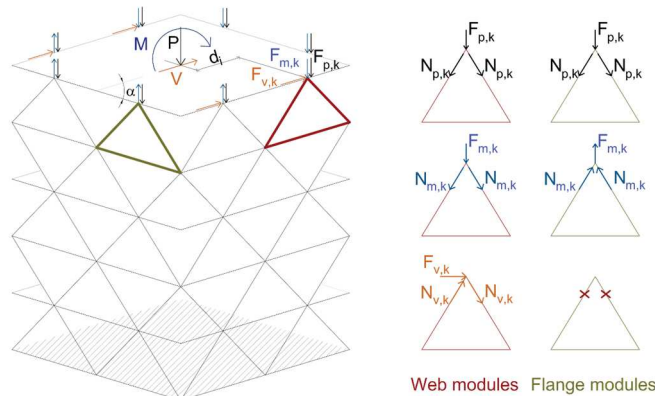


Fig. 2 Diagrid module: effect of gravity load P (associated with the diagrid self weight), overturning moment M and shear force V . Where $F_{p,k}$, $F_{m,k}$, and $F_{v,k}$ are the forces in the k -th module due to vertical load, overturning moment and the shear force, respectively; and $N_{p,k}$, $N_{m,k}$ and $N_{v,k}$ are the correspondent internal actions.

When the diagrid is subject to gravity and seismic loads, the axial force in the diagonal elements of the k -th module at the m -th floor can be calculated as follow:

$$N_k = N_{p,k} + N_{m,k} + N_{v,k} = \frac{F_{p,k} \cdot \sin(\vartheta)}{2} \pm \frac{M_m d_k \cdot \sin(\vartheta)}{\sum_{i=1}^{n_k} d_i^2} \pm \frac{V_m \cos(\alpha)_k \cdot \cos(\vartheta)}{\sum_{i=1}^{n_k} \cos(\alpha)_i} \quad (1)$$

Where, d_i is the distance of the i -th module from the whole diagrid centroid axis (Figure 2) and n_k is the total number of the modules in the whole diagrid.

Once the geometry and load pattern of the diagrid are defined, the definition of the design targets is of fundamental importance.

2.2 Stiffness constraint

The design procedure is aimed at identifying the diagonal element cross-section that satisfies all the imposed targets. In order to set the stiffness constraint, the limit target related to the existing building features and then the required minimum stiffness is identified.

In particular, in the case of post-world war RC buildings, starting from the limit inter-story drift allowed by the existing structure, the limit top displacement of the reference MDOF system can be derived as shown in Table 1.

Table 1 Correlation between the drift allowed and the top displacement.

Limit Drift	Inter-story displacement [mm]	TOP displacement [mm]	Limit Drift
θ	$\delta_i = \theta \cdot h_i$	$\delta_{TOT} = \delta_i \cdot n_{\text{floors}}$	θ

Subsequently, in order to evaluate the retrofitted structure stiffness, as suggested by Baker [10] for the structural design of tall buildings, the whole system is modeled as a cantilever beam. In the case of shear buildings subjected to seismic loads, the top displacement is equal to:

$$y(0) = \frac{8pL^2}{24A_s Gk} + \frac{11pL^4}{120EI} \quad (2)$$

where p is the distributed triangular load on the cantilever beam; E , I and A_s are the elastic module, the inertia momentum and the cross-section area of the diagonal elements, respectively; k is the Timoshenko shear coefficient, and L is the building height. Furthermore, in order to take into account the discrete nature of the diagrid [11]:

$$\begin{cases} A_s = 2n_w A_{d,w1} \cos(\vartheta) \\ I = n_f A_{d,f1} \sin(\vartheta) l^2 \end{cases} \quad (3)$$

where, n_w and n_f are the number of diagonals on the web façade and on the flange façade, respectively. $A_{d,w1}$ and $A_{d,f1}$ are the area of the diagonal elements on the web and flange façade; l is the plan direction of the building parallel to the considered seismic direction.

Therefore, by imposing the maximum displacement $y(0)$ equal to the limit top displacement, the minimum cross-section areas - $A_{d,w1}$ and $A_{d,f1}$ - that satisfy the stiffness target can be obtained.

To summarize, the first design target is to prevent excessive damage to the existing structure, thereby avoiding the long disruption of the building activities and the relocation of the inhabitants. This target represents an essential step in the design procedure and should be calibrated as a function of the reference building features. Finally, it is worth noting that the seismic load pattern is not exactly represented by a point load on each floor but with a triangular distributed load. However, this distribution simplifies the procedure considerably and does not introduce significant errors in the diagrid design.

2.3 Strength constraint

As mentioned above, the diagonal elements of the diagrid are subjected to compressive stresses and buckling may occur. Buckling is characterized by a sudden sideways deflection of the structural element and in the case of diagrid as a retrofit solution, this behavior has to be avoided.

In order to introduce the axial limit force for the diagonal elements in the design procedure, the limit axial force N_i^{LIM} of each commercial profile (NTC, 2008) is compared with the calculated internal actions N_k . In particular, it yields:

$$N_k \leq N_i^{LIM} = \frac{A_i \cdot \sigma_{LIM}}{\omega} \quad (4)$$

where A_i is the cross-section area of the i -th commercial profile, σ_{LIM} is the maximum axial stress allowed and the coefficient ω is a function of the profile slenderness.

The choice of the boundary condition of the diagrid modules and, consequently, the effective length of the diagonal elements plays a very important role in this step of the design procedure. For this reason, different configurations of the boundary conditions should be analyzed in order to optimize the diagrid solution.

Finally, the maximum cross-section area obtained from the comparison between (b) and (c) represents the final dimension of the diagrid elements. In particular, if diagonal elements of the web and the flange facades are different between, it yields:

$$\begin{aligned} A_{d,w} &= \max(A_{d,w1}, A_{d,w2}) \\ A_{d,f} &= \max(A_{d,f1}, A_{d,f2}) \end{aligned} \quad (5)$$

where, $A_{d,w}$ and $A_{d,f}$ are the area of the diagonal elements in the web and in the flange facades, respectively, as obtained from the 2 steps.

3 Application to a reference building

In order to evaluate the effectiveness of the design procedure, the procedure has been applied to a reference building. The reference structure is a post-World War II reinforced concrete building. Main features and structural details are described in [12], [13].

The structure is a five-story rectangular building (24x11mq) featuring three one-way longitudinal frames and two infilled lateral frames. The inter-story height is 3.15 m, and the structural system is made of R.C. frames in the longest direction. From a structural point of view, the building is made of a reinforced concrete structural frame designed to withstand static loads only. Beams are designed to withstand the vertical loads. Floors are made of composite RC beam and clay block system featuring a 2.5 cm RC overlay. On the basis of previous studies, it has been assumed that floors can withstand horizontal loads (i.e. they behave like floor diaphragms) by developing an in-plane tied-arch resistant mechanism up to their ultimate capacity [12], [13]. The staircase core is not designed to withstand seismic loads; accordingly, the staircase walls are not considered as RC seismic walls, but rather as stiff walls with low ductility. Geometry and materials of the main frame are reported in Figure 3.

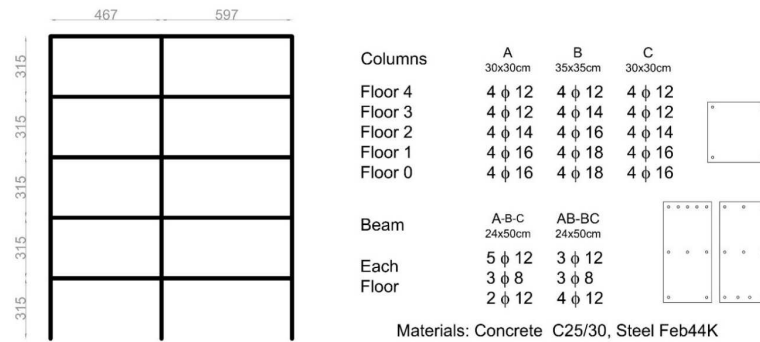


Fig. 3 Geometry and materials of the main frame.

3.1 Existing building model

The finite element model was developed with MidasGen 2015. In the existing building model, attention has been paid to the correct representation of both structural and non-structural components. Non-linear static analyses were performed in order to evaluate the structural performance of the reference building in the As-Is conditions.

Infilled walls were modeled as two non-linear equivalent trusses. In particular, for the infill panels, the cracking and peak forces were evaluated according to Decanini et al. [14], while the se-

lected cracking and peak drifts are in accordance to the traditional values of 0.5% drift for moderate damage and 1.5% drift for the infill collapse [15]. As a result, the equivalent truss dimensions are 1.372m x 0.13m for the shorter and 1.4m x 0.13m for the longer infill walls.

Once the model has been defined, non-linear static analyses were performed. The reference building was supposed to be located in L'Aquila, with C soil category and T1 topography. The capacity curve of the reference building and the displacement demands are plotted in Figure 4.

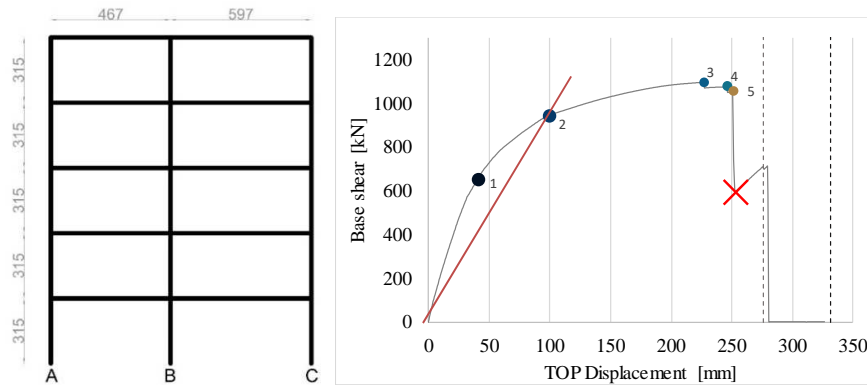


Fig. 4 Capacity curve of the existing building: 1. Infills Cracking; 2. Infills Failure; 3. Stair core limit strength; 4. Plastic hinges in the lateral columns; 5. Plastic hinges at the base of all columns. Dot line: the displacement demands at the Life Safety Limit State and Collapse Limit State; Red line: equivalent stiffness of the existing building.

As shown in figure 4, the existing building does not satisfy L'Aquila displacement demands [16] and for this reason, the renovation of the existing building is required.

3.2 Diagrid design method: application

As already specified, the retrofit is carried on from outside, in order to avoid inhabitants' relocation and it is designed with a Life Cycle Thinking approach.

In order to achieve the retrofit objectives, specific design targets were set. In particular, a maximum inter-story drift equal to 0.5% (to avoid damage) and a maximum base shear flow equal to 300 kN/m (guaranteeing feasibility of the foundation systems) were considered. Moreover, a maximum inter-story shear action of 625 kN [12], [13] was adopted to avoid retrofit of the floors (the value is evaluated based on the in-plane capacity of the floors), and beyond this limit, either the retrofit of the existing floors or external diaphragms are needed. Based on the design target choice, geometry and loads and through the stiffness and strength constraints, the design procedure led to the proportioning of the diagrid.

3.2.1 Geometry and loads

As far as the diagrid geometry is concerned, the diagrid was conceived to be in close proximity to the existing building and a module angle equal to 48° has been set. The resulting diagrid layout and geometry is shown in Figure 5. It is worth noting that the selected angle compared to the optimal angle suggested by Moon et al [5, 6] implies a 13% reduction of the diagrid module lateral stiffness; however, it is a compromise between the architectural features and the optimal angle of 35° .

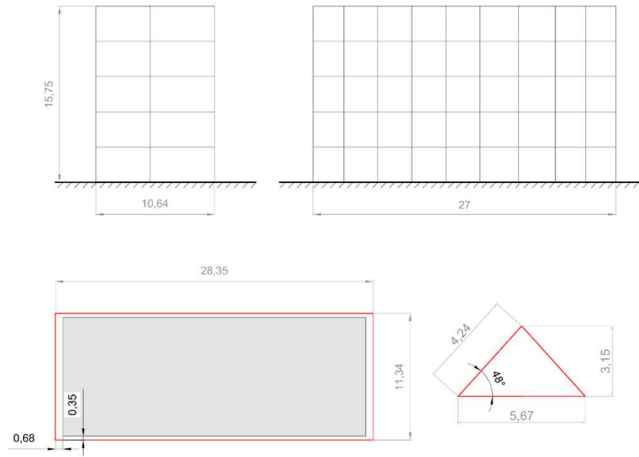


Fig. 5 Geometry and Module. In red the diagrid and in grey the existing building.

In this case, S355 tubular profiles were considered.

Once the existing building performance and diagrid features were determined (figure 5), the seismic load pattern and the diagrid module internal forces were derived. In particular, according to Eq. (1), the axial forces in each module of the diagrid were calculated:

$$N_k = N_{M,k} + N_{V,k} = \frac{M_m d_k}{\sum_{i=1}^{n_k} d_i^2} \cdot \frac{\sin(\vartheta)}{2} \pm \frac{V_m \cos(\alpha)_k}{\sum_{i=1}^{n_k} \cos(\alpha)_i} \cdot \frac{\cos(\vartheta)}{2} \quad (6)$$

It should be pointed out that, in this case, the vertical loads of the diagrid were neglected because their magnitude was negligible.

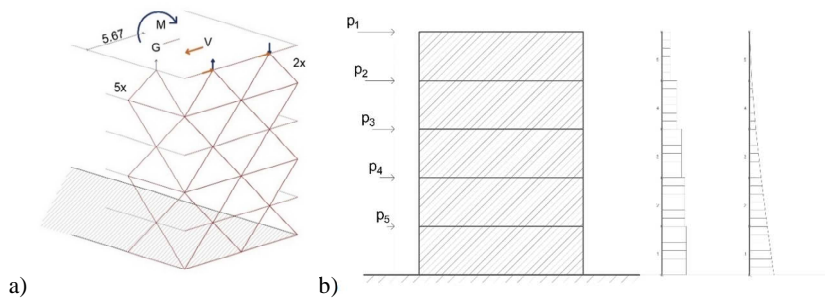


Fig 6 a) Forces in the diagrid module and b) Load pattern of the whole system.

The maximum base shear of the diagrid and, consequently, p_i were derived by setting the target displacement for the equivalent SDOF system u_N , in accordance with Mehrabi and Shing[17]:

$$\begin{aligned} M_e &= \{1\}^T \mathbf{M} \{\Phi\} \\ k_E &= \frac{4\pi^2 M_e}{(T)^2} \\ V &= k_E \cdot u_N \end{aligned} \quad (7)$$

where M is the mass matrix of the whole system, k_E and T are the effective stiffness and the effective period of the system, respectively, and V_1 is the total base shear.

Is it worth mentioning that, in order to derive the diagrid base shear, an equivalent stiffness of the structure was taken into account according to the limit target set (figure 5) and an iterative procedure was adopted in order to take into account the real mass of the external diagrid.

3.2.2 Maximum stiffness

As mentioned, the stiffness constraint objective is to avoid extended damages on the existing building. For this reason, an inter-story drift limit of 0.5% was adopted. Therefore, supposing that the system behaves like a cantilever beam subjected to a distributed triangular load, the maximum displacement of the retrofitted structure was calculated as indicated in (2) and (3):

$$y(0) = \frac{8pL^2}{24A_sGk} + \frac{11pL^4}{120EI} \quad \left\{ \begin{array}{l} A_s = 2n_W A_{d,W} \cos(\vartheta) \\ I = n_f A_{d,f} \sin(\vartheta) l^2 \end{array} \right.$$

where, for the reference structure:

$$\begin{aligned} p &= 2 \cdot V_D / L \\ L &= 15.75[m] \\ \vartheta &= 48^\circ \\ n_W &= 4 \\ n_f &= 10 \\ l &= 11.34[m] \end{aligned}$$

By imposing $y(0)$ equal to the target displacement:

$$0.5 \cdot L = \frac{8pL^2}{24A_sGk} + \frac{11pL^4}{120EI} \quad (8)$$

the cross-section area of the diagonal element of the diagrid (A_s) has been calculated. In addition, by imposing a tubular thickness of 10 mm, the element diameter could be determined. Therefore, the enforcement of the stiffness constraint results in:

$$\left\{ \begin{array}{l} \Phi_1 = 108.41 \text{ mm} \\ s_1 = 10.0 \text{ mm} \end{array} \right.$$

3.2.3 Maximum axial load

Finally, in order to avoid buckling of the elements and to meet the strength limit constraint, the second minimum profile has been determined by combining the maximum axial force of the elements and the maximum capacity of the commercial profiles as shown in Figure 7.

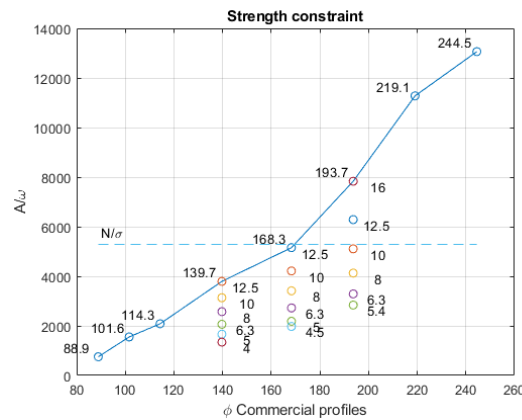


Fig. 7 Green line: Target; Blue line: Commercial profile ratio A/ω , Circles represent the ratio A/ω changing the profile thickness.

In this case:

$$\begin{cases} \Phi_2 = 193.7 \text{ mm} \\ s_2 = 12.5 \text{ mm} \end{cases}$$

At this point, the design profile diameter was derived as the maximum between Φ_1 and Φ_2 :

$$\begin{cases} \Phi_{Fin} = 193.7 \text{ mm} \\ s_{Fin} = 12.5 \text{ mm} \end{cases}$$

3.2.4 Time history analysis

In order to validate the diagrid design procedure for shear-type buildings, 7 non-linear Time History analyses were carried out. Accelerograms compatible with the code spectrum were determined by adopting the software Rexel 2.2beta [18]. A maximum scale factor equal to 2 and an upper and lower tolerances equal to 10% and 15% were imposed. It is worth noting that for the selected accelerograms the lower tolerance limit imposed by the Eurocode [19] is not met. However such a requirement is not always satisfied in the case of high seismicity areas; for this reason, a lower tolerance limit was obtained by increasing the value by 5% starting from the limit suggested by the code until a compatible set was identified [20]. Time History results, expressed in terms of total base shear, base shear at the base of the diagrid, maximum axial force in the diagonal element and top displacement are reported in Table 2.

Table 2 V_{MAX} [kN]: Total base shear; V'_{MAX} [kN]: Base shear at the base of the diagrid (no ex Building); F_{MAX} [kN]: Maximum axial force in the diagonal element; D_{TOP} [m]: Top displacement.

Accelerograms	V_{MAX} [kN]	V'_{MAX} [kN]	F_{MAX} [kN]	D_{TOP} [m]
000133_xa	6643.4	6096.5	1553.2	0.054
000355_ya	8375.7	8079.2	2077.8	0.075
000592_xa	4751.2	4262.3	1002.7	0.033
000600_xa	8528.7	7637.2	1959.1	0.072
000879_ya	7510.8	6686.3	1691.9	0.063
001726_xa	10085.7	9183.1	2374.5	0.085
001726_ya	10954.0	9766.7	2531.0	0.090
Average	8172.86	7387.33	1884.31	0.067

Results show that both the limit top displacement target of 0.0785 (m) and the maximum inter-story drift target are met (Figure 9a), except in the case of the accelerograms 001726_xa and 001726_ya. These results are reasonable because of the values of the pseudo-acceleration of those two accelerograms in correspondence of the retrofitted building period (0.5 s) are significantly higher than the target spectrum (1.22 times).

Finally, hand-calculation predictions, evaluated in accordance with the design procedure described, are very close to the model results as shown in Table 3; therefore, the value of the maximum axial force of the diagonal element derived in the first step of the design procedure is accurate and the commercial profile choose can satisfy the demand.

Table 3 V_{MAX} [kN]: total base shear; V'_{MAX} [kN]: Base shear at the base of the diagrid (no ex Building); F_{MAX} [kN]: Maximum axial force in the diagonal element; D_{TOP} [m]: Top displacement.

Accelerograms	V_{MAX} [kN]	V'_{MAX} [kN]	F_{MAX} [kN]	D_{TOP} [m]
Average	8172.86	7387.33	1884.31	0.0670
Hand C.	8169.70	7249.30	1876.80	0.0787

δ_{error}	-	-1.87%	-0.6%	+15%
------------------	---	--------	-------	------

The total base shear of the diagrid of 7387 kN corresponds to a base shear flow of 325 kN/m; this result could be considered acceptable because only slightly higher than the imposed limit value. Finally, concerning the inter-story shear the adopted limit value is exceeded, therefore external diaphragms should be introduced, as shown in Figure 9b.

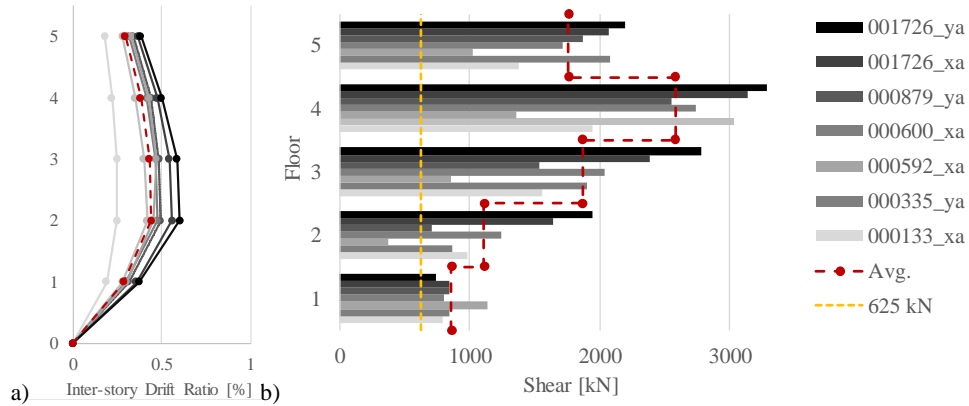


Fig. 9 a) Average inter-story drift and b) floor shear along the building height for different solutions.

4 Concluding remarks

This work is part of an ongoing research on the holistic renovation of the post-WWII RC buildings. In particular, a design procedure for the proportioning of diagrid exoskeletons to be adopted as seismic mitigation measures was proposed in this paper. The procedure takes into account both the existing building and the diagrid performances, limits and features. Starting from the geometry and loads criterion, through the minimum stiffness requirement and to the maximum allowable axial force, the minimum profile for the diagrid can be obtained. The effectiveness of the method was assessed through the application of the procedure to a reference building. The study showed that the maximum strength limit governs the procedure in the case of the reference shear-type building.

In the future step of the research, a much wider range of buildings, having different characteristics and features, will be examined and a sensitivity analysis will be carried out to detect the most critical parameters influencing the diagrid proportioning.

References

- [1] Belleri, A., & Marini, A. (2016). Does seismic risk affect the environmental impact of existing buildings? *Energy and Buildings*, 110, 149-158. doi:10.1016/j.enbuild.2015.10.048.
- [2] Economidou, M., Lausten, J., Ruyssevelt, P., & Staniaszek, D. (2011). *Europe's Buildings Under the Microscope* (Rep.). Buildings Performance Institute Europe (BPIE).
- [3] FEMA398, "FEMA 398 Incremental Seismic Rehabilitation of Multifamily Apartment Buildings. Risk management series." 2004.
- [4] European Climate Foundation. (2010). *Roadmap 2050: a practical guide to a prosperous, low- carbon Europe Volume I: technical and economic assesment*, I, 387. <https://doi.org/10.2833/10759>.
- [5] Labò, S., Passoni, C., Marini, A., Belleri, A., Camata, G., Riva, P., & Spacone, E. (2017). Prefabricated Responsive Diagrids for Holistic Renovation of Existing Mid-Rise Rc Buildings. In *Proceedings of the 6th International Conference on Computational Methods in Structural Dynamics and Earthquake Engineering (COMPdyn 2017)*, Rhodes island, Greece, 15-17 June 2017.
- [6] Moon, K. S. (2008). *Practical Design Guidelines for Steel Diagrid Structures*. Aei 2008. doi:10.1061/41002(328)34.
- [7] Moon, K., Connor, J. J., & Fernandez, J. E. (2007). Diagrid structural systems for tall buildings: Characteristics and methodology for preliminary design. *The Structural Design of Tall and Special Buildings*, 16(2), 205-230. doi:10.1002/tal.311.
- [8] Maqhareh, M. R. (2014). *The Evolutionary Process of Diagrid Structure Towards Architectural, Structural and Sustainability Concepts: Reviewing Case Studies*. *Journal of Architectural Engineering Technology*, 03(02). doi:10.4172/2168-9717.1000121.
- [9] Montuori, G. M., Mele, E., Brandonisio, G., & Luca, A. D. (2013). Design criteria for diagrid tall buildings: Stiffness versus strength. *The Structural Design of Tall and Special Buildings*, 23(17), 1294-1314. doi:10.1002/tal.1144.
- [10] Baker, W. F. (2013). *The Tall Buildings Reference Book*. doi:10.4324/9780203106464.
- [11] Mele, E., Fraldi, M., Montuori, G. M., & Perrella, G. (2016). Non-conventional Structural Patterns for Tall Buildings : from Diagrid to Hexagrid and Beyond Non-conventional Structural Patterns for Tall Buildings : from Diagrid to Hexagrid and Beyond. In *Fifth International Workshop on Design in Civil and Environmental Engineering*, Sapienza University of Rome Representative, October 6-8, 2016.
- [12] Feroldi, F. (2014). *Sustainable renewal of the post WWII building stock through engineered double skin, allowing for structural retrofit, energy efficiency upgrade, architectural restyling and ur-ban regeneration*. PhD Thesis, University of Brescia (In Italian).
- [13] Passoni, C. (2016). *Holistic renovation of existing RC buildings: a framework for possible integrated structural interventions*. PhD Thesis, University of Brescia.
- [14] Decanini, L., Mollaioli, F., Mura, A., & Saragoni, R. (2004). Seismic Performance of Masonry Infilled R/C Frames. *13th World Conference on Earthquake Engineering*, (165), Paper No. 165.
- [15] A. B. Mehrabi, P. B. Shing, M. P. Schuller, and James L. Nolan, "Experimental Evaluation of Masonry-Infilled RC Frames. *Journal of Structural Engineering*, 122(3), 228-237. [https://doi.org/10.1061/\(ASCE\)0733-9445\(1996\)122:3\(228\)](https://doi.org/10.1061/(ASCE)0733-9445(1996)122:3(228)).
- [16] "D.M. 14/01/2008, 'Norme Tecniche per le Costruzioni (NTC 2008)', *Gazzetta Ufficiale*, n. 29 del 14/02/2008, Supplemento ordinario n.30. (in Italian)."
- [17] Mehrabi, A. B., & Shing, P. B. (2003). Seismic analysis of masonry infilled reinforced concrete frames. *Masonry Soc. J.*, 81-94.
- [18] Iervolino, I., Galasso, C., & Cosenza, E. (2009). REXEL: Computer aided record selection for code-based seismic structural analysis. *Bulletin of Earthquake Engineering*, 8(2), 339-362. doi:10.1007/s10518-009-9146-1.
- [19] "[Eurocode 8]: CEN, 'European Standard EN 1998-2005 Eurocode 8: Design of structures for earthquake resistance', European Committee for Standardization, Brussels, Belgium."
- [20] Iervolino, I., Galasso, C., & Cosenza, E. (2008). REXEL 2.2 beta: uno strumento per la selezione di accelerogrammi naturali per le NTC e l'Eurocodice 8. XVII Congresso CTE.